

Strain-Balanced Silicon-Germanium Materials for Near IR Photodetection in Silicon-Based Optical Interconnects

by

Laura Marie Giovane

S.B., Materials Science and Engineering
Massachusetts Institute of Technology, 1993

Submitted to the Department of Materials Science and Engineering
in partial fulfillment of the requirements for the Degree of
Doctor of Philosophy in Electronic Materials

at the

MASSACHUSETTS INSTITUTE OF TECHNOLOGY

June 1998

© 1998 Massachusetts Institute of Technology
All rights reserved

Author

Department of Materials Science and Engineering
May 1, 1998

Certified by

Lionel C. Kimerling
Thesis Supervisor
Thomas Lord Professor of Materials Science and Engineering

Certified by

Eugene A. Fitzgerald
Thesis Supervisor
Associate Professor of Materials Science and Engineering

Accepted by

Linn W. Hobbs
John F. Elliot Professor of Materials
Chair, Departmental Committee on Graduate Students

ARCHIVES

AUG 17 1998

LIBRARIES

Chapter 4

Optical Performance

For photodetector design the single most important material property is the absorption coefficient. Simply, a material must absorb light before it can detect it. The absorption coefficient is therefore the critical device design parameter for high quantum efficiency photodetectors. Optimization of the absorption coefficient maximizes the percentage of carriers created in the active region of a device. Light incident on a material with an absorption coefficient much greater than the design optimum may create most or all of the photogenerated carriers near the surface, where they are likely to recombine. Conversely, a material with an absorption coefficient that is too low will not absorb a significant fraction of the incident photons.

The absorption coefficients of silicon-germanium alloys at $\lambda=1.3$ and $1.55\mu\text{m}$ are lower than optimum. Thus, achieving high quantum efficiency germanium-silicon photodetectors requires maximization of the absorption coefficient. While the absorption spectra of pure silicon and germanium are well known, and pioneering work by Braunstein *et al.*⁶⁵ reported the absorption spectrum of relaxed silicon-germanium alloys, little, if any, data is available about the absorption coefficient of strained silicon-germanium alloys.

Maximizing the absorption coefficient requires an understanding of, and an ability to manipulate a material's electronic band structure. In the case of silicon-germanium alloys, two "handles" are available by which to manipulate the band structure: alloy composition and strain. Although the effect of alloy composition and strain on band gap has been addressed for the limited case of silicon-germanium alloys strained coherently on silicon substrates, the combined effect of strain and composition on band gap and the absorption coefficient have not.

In this chapter, a model is presented which calculates the band gap and the absorption coefficient as a function of strain and composition. The model is based on the critical points in the relaxed band structure and uses deformation potential theory to calculate how these critical points shift with biaxial $\langle 001 \rangle$ strain. The absorption coefficient is calculated for each transition between the valence band maxima and the local conduction band minima. Spectral photocurrent response of the strain-balanced superlattice materials has been measured and a comparison to the model is made.

Section 4.1 details the band structure of pure silicon, pure germanium, and silicon-germanium alloys. The effects of biaxial strain on the lattice and the band structure are detailed in Section 4.2. A discussion of the how strain and alloy composition affects the band gap is also included. Section 4.3 sets forth the basic principles of determining the absorption coefficient from knowledge of the band structure. An outline for the model that calculates absorption coefficient as a function of wavelength, biaxial (100) strain and alloy composition is presented in Section 4.3.4. In Section 4.4, the photocurrent response of strain-balanced superlattice photodetectors is presented and compared to the results of the absorption model.

4.1 Band Structure

An ideal semiconductor band structure at 0K is characterized by a completely filled valence band and a completely empty conduction band; the two are separated by a band gap, in which there are no allowable states. Photons incident upon the ideal semiconductor will not be absorbed unless they possess energy greater than the band gap energy, the minimum level of energy required to excite electrons from the valence band

into the conduction band. To quantify the probability of such absorption events for a given semiconductor, the nature of that semiconductor's energy-momentum, or $E-k$, relationship must first be analyzed.

4.1.1 Conduction Band

The energy-momentum relationships for silicon and germanium are shown in Figure 4-1. Both of these semiconductors are categorized as indirect gap semiconductors because the transition from the energy maximum in the valence band to the energy minimum in the conduction band does not conserve momentum unless a third particle, such as a phonon, is emitted or absorbed. This band structure is in contrast with that of direct gap semiconductors, in which the linear momentum of an electron is the same at the conduction band minimum as the valence band maximum. The band gap of both silicon and germanium is indirect, because for both materials the conduction band minimum is not at $k=0$.

The band gaps of silicon and germanium at 300K are 1.125 and 0.67 eV, respectively. However, the band gap of silicon-germanium alloys is not a linear function of alloy composition. The non-linearity arises from the differently directed momentum vectors of the conduction band minima. The conduction band minimum of silicon lies along the six (100) directions or X-valley. And the conduction band minimum of germanium lies along the eight (111) directions or L-valley. Figure 4-2 shows the band gap of relaxed silicon-germanium alloys as a function of germanium fraction, x . For alloys with germanium fraction less than 0.85, the band structure resembles that of silicon; the conduction band minimum lies in the (100) directions or X-valleys. For alloys with germanium fraction greater than 0.85, the band structure resembles that of germanium; the conduction band minimum lies in the (111) directions or L-valleys.

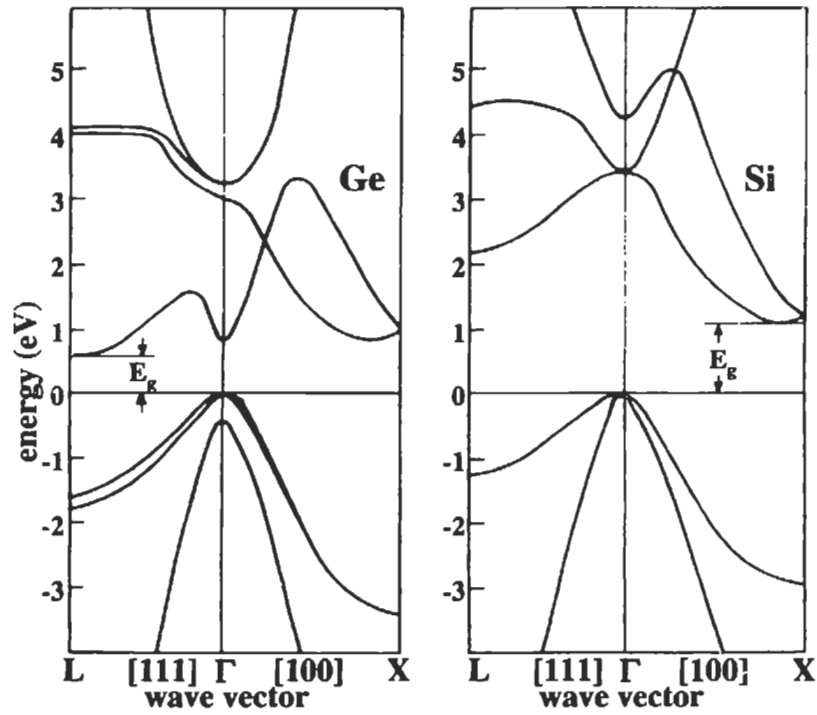


Figure 4-1: Band structure of germanium and silicon. The conduction band minimum for germanium lies in the [111] and for silicon in the [100].⁶⁶

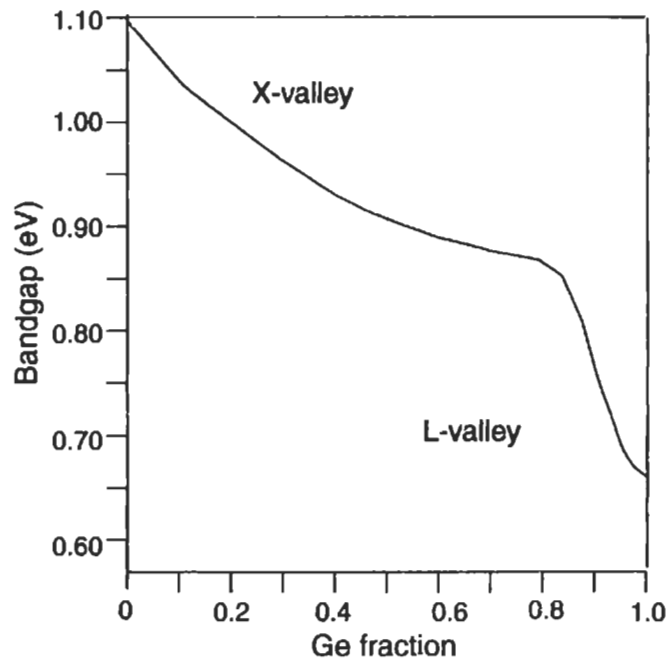


Figure 4-2: Band gap of relaxed silicon-germanium alloys as a function of germanium fraction, x

4.1.2 Valence Band

The valence band of silicon is composed of p-like bonding state with a maximum energy at $k=0$. The valence band maximum consists of three, two-fold spin degenerate, bands. There are the two degenerate ($j=3/2, m_j=\pm 1/2$) and ($j=3/2, m_j=\pm 3/2$) bands and a spin-orbit split band ($j=1/2, m_j=\pm 1/2$). The spin-orbit splitting energy for silicon is 0.044 eV. Germanium's valence band structure is similar to silicon's with spin orbit splitting energy, 0.29 eV.

4.2 Strain and Band Structure

The band structure of a semiconductor is fundamentally tied to the periodicity of the semiconductor's lattice. Any strain in the lattice will distort the periodicity of the lattice, and will correlate to a change in the band structure. The 4% lattice mismatch between silicon and germanium lattices gives rise to a biaxial strain in the (100) for coherent silicon-germanium films grown on (100) substrates. This biaxial strain in the (100) has several effects on the band structure of silicon, germanium and their alloys, among which is a change in transition energies and the band gap energy. Deformation potential theory describes the change in energy of critical points in the band structure with respect to the strain tensor. The discussion of deformation potential theory below is adapted from the treatments by R. People⁶⁷ and F. Pollak.⁶⁸

4.2.1 Distortion Components

The distortion of a diamond cubic lattice under biaxial strain in the (100) plane can be separated into two components: tetragonal distortion and dilation distortion. Tetragonal distortion destroys the cubic symmetry of the lattice, as seen in Figure 4-3. The degree of tetragonal distortion is referred to as the tetragonal strain, e_T , and is expressed as

$$e_T = e_{||} - e_{\perp} \quad (4-1)$$

where $e_{||}$ is the in-plane strain and e_{\perp} is the out-of-plane strain. For biaxial strain in the (100), the tetragonal strain is reduced to a function of $e_{||}$ by substituting standard elastic constant relationships:

$$e_T = e_{11} \left(\frac{-2c_{12}}{c_{11}} - 1 \right) \quad (4-2)$$

where c_{11} and c_{12} are the applicable elastic constants. Tetragonal distortion impacts the band structure of silicon in two significant ways, splitting the X-valley conduction band and the splitting valence band. Dilation distortion is the fractional change in volume under strain. This change in volume can be expressed in terms of elastic constants and the in-plane strain as:

$$\frac{\Delta V}{V} \equiv e_{11} \left(\frac{-2c_{12}}{c_{11}} + 2 \right) \quad (4-3)$$

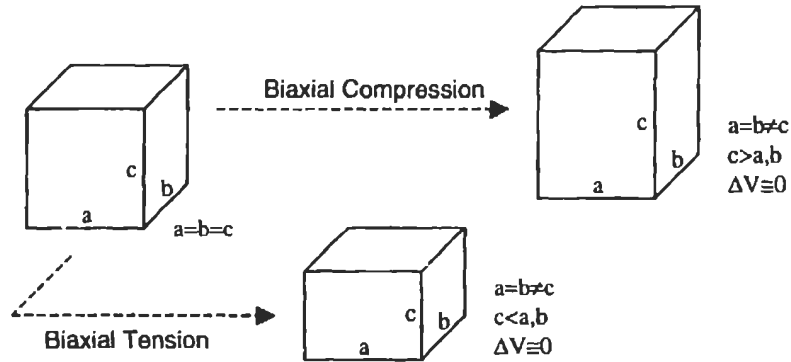


Figure 4-3: Tetragonal Distortion

4.2.2 Conduction Band Splitting

Biaxial strain in the (100) splits the energy of the six-fold degenerate X-valley conduction band minima, resulting in what is commonly referred to as a doublet and a singlet, (although quartet and doublet might actually better describe the strain-split six-fold degenerate minima better). The conduction band splitting energies for the singlet and doublet, ΔE_c^s and ΔE_c^d , due to biaxial strain in the (100) are given by:

$$\Delta E_c^s = -\frac{2}{3} E_2 e_T, \text{ for } (100) \text{ and } (\bar{1}00) \text{ valleys} \quad (4-4)$$

$$\Delta E_c^d = \frac{1}{3} E_2 e_T \text{ for } (010), (001), (0\bar{1}0), \text{ and } (00\bar{1}) \text{ valleys,} \quad (4-5)$$

where E_2 is the X valley conduction band deformation potential, $E_2=(-9.2)$ eV for silicon.⁶⁹

4.2.3 Valence Band Splitting

In describing the shifts of the valence band with strain, the nomenclature of the three bands is sometimes changed to ν_1 , ν_2 , and ν_3 to account for the coupling of $j=3/2$, $m_j=\pm 1/2$ and $j=1/2$, $m_j=\pm 1/2$ spin orbit band. Thus ν_1 and ν_3 represent a linear combination of the $j=1/2$, $m_j=\pm 1/2$ band and the $j=3/2$, $m_j=\pm 1/2$ band. The $j=3/2$, $m_j=\pm 3/2$ band does not couple and corresponds directly to ν_2 .

The splittings in valence band energies arise from the tetragonal distortion; the change in energies, $\Delta E_{\nu_1}^s$, $\Delta E_{\nu_2}^s$ and $\Delta E_{\nu_3}^s$, are given by:

$$\Delta E_{\nu_2}^s = -e_T b \quad (4-6)$$

$$\Delta E_{\nu_1}^s = \frac{1}{2} \left[(\Delta_0 + e_T b) - \sqrt{\Delta_0^2 - 2\Delta_0 e_T b + 9e_T b} \right] \quad (4-7)$$

$$\Delta E_{\nu_3}^s = \frac{1}{2} \left[(\Delta_0 + e_T b) + \sqrt{\Delta_0^2 - 2\Delta_0 e_T b + 9e_T b} \right] \quad (4-8)$$

where b is the valence band shear deformation potential for (100) distortions, with $b_{si}=(-2.2)$ eV and $b_{ge}=(-2.6)$ eV,⁶⁹ and where Δ_0 is the spin orbit split energy.

4.2.4 Hydrostatic Shift

The dilation distortion shifts the valence and conduction bands with respect to one another. This shift is referred to as the hydrostatic shift because this kind of deformation in the band structure is observed under hydrostatic pressure. It should be noted that the dilation distortion does not diminish the high order symmetry of the diamond cubic lattice and hence no splitting of the otherwise degenerate bands results from this contribution. The hydrostatic energy shift ΔE_g^H is:

$$\Delta E_g^H = (E_1 + a_1) \frac{\Delta V}{V}, \quad (4-9)$$

where (E_I+a_I) is the hydrostatic pressure deformation potential, $(E_I+a_I)=1.6$ for silicon and $(E_I+a_I) =(-5.7)$ for germanium.⁶⁹ The hydrostatic deformation potential for silicon is positive. Thus, a decrease in volume leads to a small band gap. Germanium however has a negative deformation potential and thus, a decrease in volume leads to a larger band gap.

4.2.5 Band gap as a Function of Strain and Composition

Figure 4-4 shows the band gap as a function of germanium fraction x for relaxed silicon-germanium alloys and the band gap of silicon-germanium alloys strained coherently to the silicon lattice as calculated by R. People.⁶⁷ For coherently strained silicon-germanium alloys on silicon substrates, biaxial strain is a function of germanium fraction:

$$e_{11} = -0.042x, \quad (4-10)$$

where x is the germanium fraction. Because the strain-balanced superlattice permits composition and strain to be varied independently it is useful to calculate the band gap of silicon-germanium alloys as a function of strain and composition.

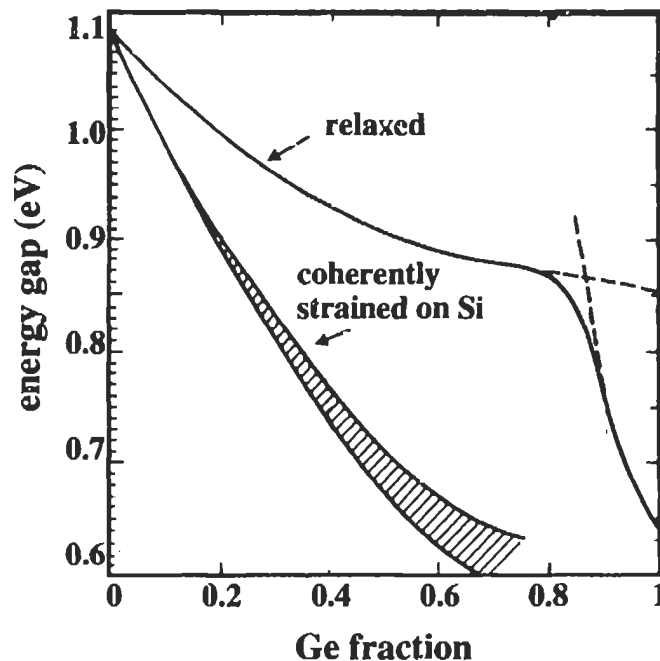


Figure 4-4: Band gap as a function of germanium fraction x for relaxed silicon-germanium alloys and the band gap of silicon-germanium alloys strained coherently to the silicon lattice, as calculated by R. People.⁶⁷

The strain perturbed band gap can be determined by considering the contributions of each strain-split band in the conduction band and valence band. Figure 4-5 shows each of the deformation potential contributions as a function of biaxial strain in the (100) for silicon. The calculation of the minimum band gap of a strained silicon-germanium alloy depends on whether the conduction band minimum lies in the L or X valley. The following equations describe the change in band gap:

$$\Delta E_g^X = \Delta E_g^H + \Delta E_c^s + \Delta E_{v_1}, \quad (4-11)$$

for biaxial tension, X-valley conduction band minimum;

$$\Delta E_g^L = \Delta E_g^H + \Delta E_{v_1}, \quad (4-12)$$

for biaxial tension, L-valley conduction band minimum;

$$\Delta E_g^X = \Delta E_g^H + \Delta E_c^d + \Delta E_{v_1}, \quad (4-13)$$

for biaxial compression, X-valley conduction band minimum and

$$\Delta E_g^L = \Delta E_g^H + \Delta E_{v_2}, \quad (4-14)$$

for biaxial compression, L-valley conduction band minimum,

where ΔE_g^X and ΔE_g^L denote the change in band gap for a conduction band minimum lying in the X- and L- valley respectively. The change in the direct gap transition energy is equivalent to the change in band gap for an L-valley conduction band minimum.

To determine the band gap energy of a silicon-germanium alloy as a function of biaxial strain in the (100) and composition, the relaxed band gap of silicon-germanium alloys should be added to the change in band gap energy from the appropriate equation above.

The relaxed band gap of silicon-germanium alloys has been studied extensively and can be expressed mathematically as:⁷⁰

$$\Delta E_g^X(x) = 1.1 - 0.43x + 0.206x^2 \quad (4-15)$$

$$\Delta E_g^L(x) = 1.934 - 1.270x \quad (4-16)$$

where x is the germanium fraction. To describe the changes in band gap with respect to strain, the deformation potential constants, the elastic moduli and the spin orbit splitting energy are linearly interpolated as a function of the germanium fraction. The exception is

the conduction band deformation potential, which describes how the conduction band splits with respect to tetragonal distortion. Because the (100) local conduction band is considerably higher energy than both the (111) minimum and the direct gap local minima in germanium bulk material, a value for its deformation potential is not available in the literature. For this calculation of the strain perturbed band structure it has been assumed that the conduction band splitting deformation potential is independent of alloy composition. The C code used to determine the band gap as a function of strain and composition is included in Appendix A.

The band gap as a function of strain and composition is shown in Figure 4-6. The curves show iso-band gap energies for composition (ordinate) and biaxial strain in the (100) (abscissa). The resemblance of these curves to a topological map has led to the term band gap map to describe them. The ridges for non-strained alloys $e_{ij}=0$ represents the relaxed band gap as shown in Figure 4-2. For alloys with germanium fraction less than 0.85, the band gap is a strong decreasing function with strain, irrespective of sign. The strong dependence on strain arises from the significant conduction band minima splitting which dominates the other contributions. For alloys with germanium fraction greater than 0.85, the sign of the hydrostatic contribution term ensures that the band gap is reduced in the tensile case. For compression, however, the situation is more complicated. Where the germanium fraction x equals 0.85, the band structure of relaxed alloys is degenerate at both the (111) L-valley and the (100) or X-valley. The application of biaxial compressive strain causes the transition energy between the valence band maximum and the L-valley to increase and the valence band maximum and the X-valley to decrease. Thus, the germanium fraction at which the X-valley conduction band minimum and L-valley conduction band minimum are degenerate is a function of biaxial strain. The ledge-like discontinuity in the band gap map at high germanium fractions represents the transition between a conduction band minimum which lies in the L-valley and one that lies in the X-valley.

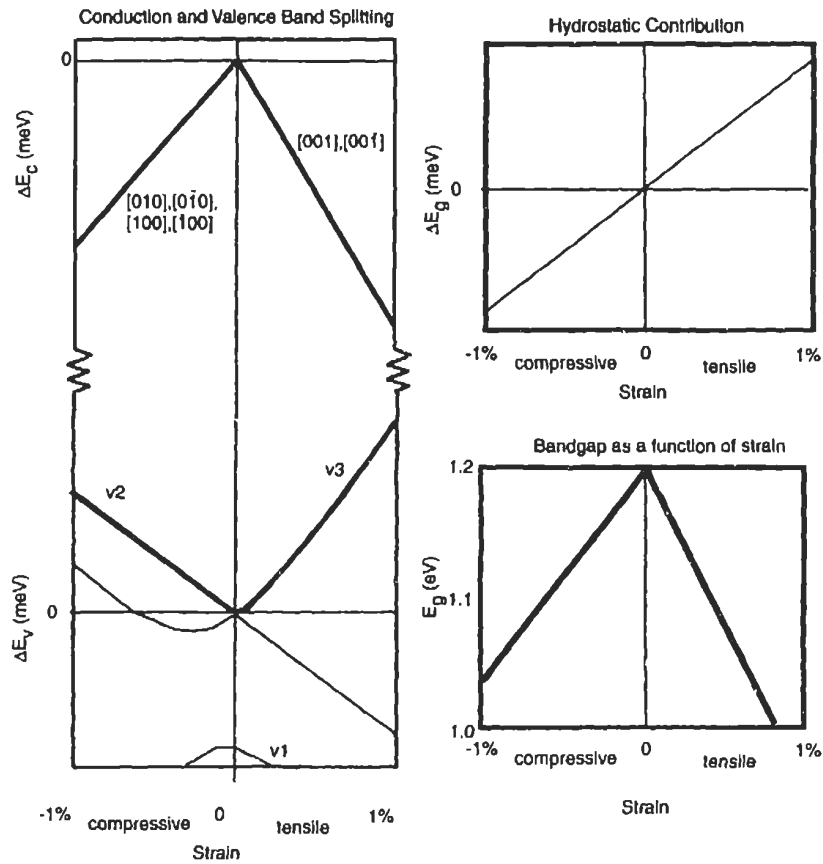


Figure 4-5: Summary of contributions to band structure changes for silicon under biaxial strain in the (100). [Left] shows the splitting of the conduction band minima and the valence band at $k=0$. [Topright] shows the change in band gap due to the hydrostatic contribution. [Bottomright] shows the sum of the three contributions on the overall band gap.

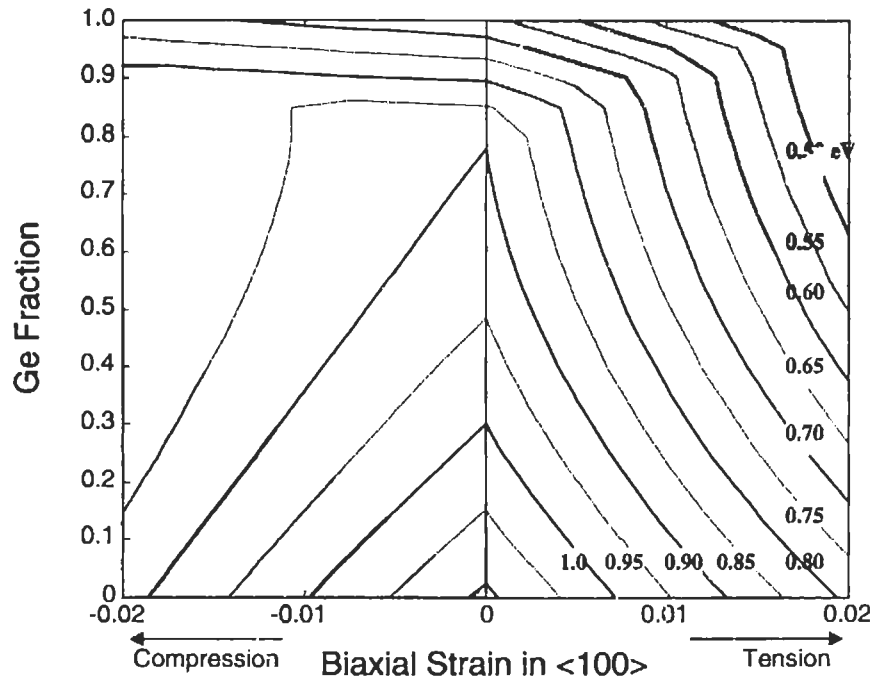


Figure 4-6: Band gap as a function of composition and strain, calculated using deformation potential theory. Unshaded areas are strain and compositions achievable using a strain-balanced superlattice structure.

4.3 Absorption

The band gap energy marks the absorption edge for indirect gap semiconductors. The onset of absorption is weak for photons with energies just larger than the band gap. Figure 4-7 shows the absorption spectrum for bulk silicon and germanium. The absorption coefficient at the band gap is weak ($\alpha < 10 \text{ cm}^{-1}$) until the photon energy is significantly greater than the band gap energy. Although the dependence of the absorption coefficient on alloy composition has been well-described for relaxed silicon-germanium alloys, the effect of strain on the absorption coefficient, however, has not been described. This section constructs a model that uses the deformation potential theory outlined in Section 4.2 and fundamental absorption physics to model the absorption coefficient as a function of both strain and composition.

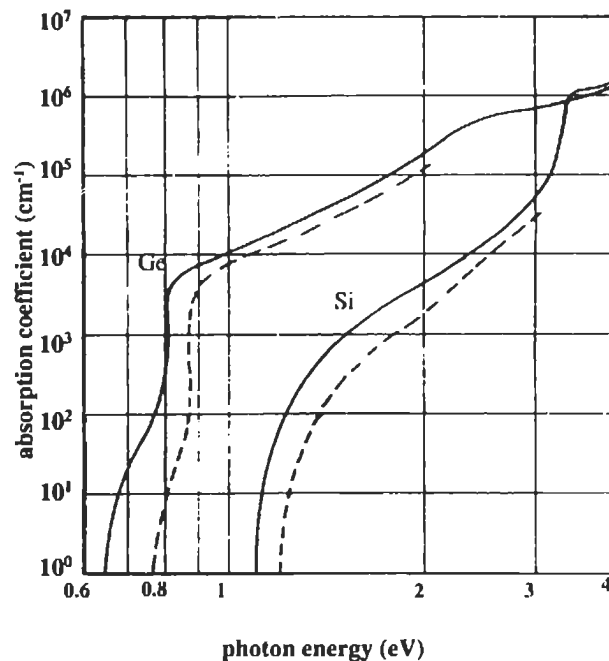


Figure 4-7: Absorption spectra for bulk silicon and germanium, solid line at 300K and dashed line at 77K.⁷¹

4.3.1 Absorption Physics

Absorption involves the interaction of a photon and electron. As the result of the interaction the photon is absorbed and the electron is excited into a higher energy state. The probability of such an interaction is described by the material's absorption

coefficient, which is mathematically defined as the relative rate of decrease in light intensity, $I_{h\nu}$ along its propagation direction:

$$\alpha_{(h\nu)} = \left(\frac{1}{I_{(h\nu)}} \right) \frac{dI_{(h\nu)}}{dx} \quad (4-17)$$

The absorption coefficient for a given photon energy, $h\nu$, is proportional to the probability P_{if} for the transition from the initial to final state and to the density of electrons in the initial state, n_i , and the density of empty states, n_f . The absorption coefficient is defined as the summation of these factors over all possible transitions:⁷²

$$\alpha_{h\nu} = A \sum P_{if} n_i n_f, \quad (4-18)$$

where A is a proportionality constant. In determining the density of initial and final states for a given transition, the requirements of conservation of energy and momentum apply.

This section addresses three fundamental transitions: 1) direct transitions between the valence band minimum and the $k=0$ conduction band extremum, 2) indirect transitions involving the emission of a phonon and 3) indirect transitions with phonon absorption.

4.3.2 Absorption Coefficient: Direct Transitions

Momentum conserving transitions between the $k=0$ valence band maximum and the $k=0$ local conduction band minimum are represented in Figure 4-8. Every initial state at E_i is associated with a final state E_f such that $h\nu = E_f - E_i$. If parabolic bands (constant effective masses) are assumed then the energy-momentum relationship in the conduction band is described by

$$E_f - E_g = \frac{\hbar^2 k^2}{2m_e^*} \quad (4-19)$$

and the energy-momentum relationship in the valence band is

$$E_i = \frac{\hbar^2 k^2}{2m_h^*}, \quad (4-20)$$

where m_e^* and m_h^* are the electron and hole effective density of states masses. A full derivation is presented elsewhere⁷² yielding the absorption coefficient associated with momentum conserving direct gap transitions:

$$\alpha_{direct}(h\nu) = A\sqrt{h\nu - E_g} \quad (4-21)$$

where A^* is approximately $10^4 \text{ cm}^{-1} \text{ eV}^{-1/2}$, and E_g and $h\nu$ are expressed in terms of eV. The direct transition represents the strongest absorption mechanism. Unfortunately for efforts to achieve strong absorption at longer wavelengths, the direct gap energy is over 1 eV at low and even moderate germanium fractions. For pure germanium the direct transition is at 0.80 eV. Thus high germanium fractions ($x > 0.9$) are needed for $1.3 \mu\text{m}$ (0.95 eV) light to be absorbed across the direct gap.

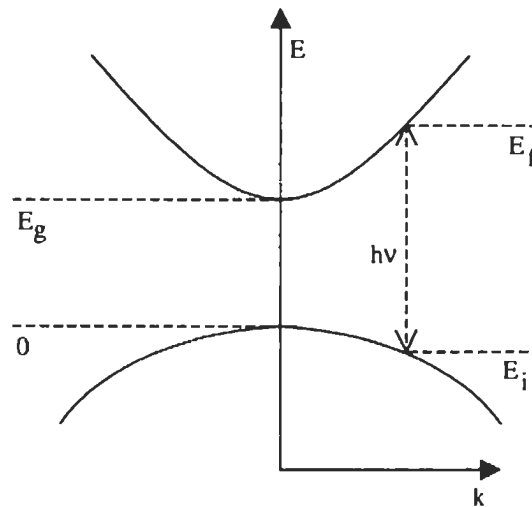


Figure 4-8: Momentum-conserving transitions between the $k=0$ valence band maximum and the $k=0$ conduction band minimum.

4.3.3 Absorption Coefficient for Indirect Transitions

For indirect transitions photon absorption involves a phonon (lattice vibration) so that momentum is conserved. Although a broad spectrum of phonons is available usually only the longitudinal or transverse acoustic phonons are involved as they have the appropriate dispersion curve to conserve momentum.⁷² Momentum conserving phonons can either be absorbed or emitted; a schematic is shown in Figure 4-9. For absorbed phonons, the energy balance is:

$$h\nu = E_f - E_i - E_p, \quad (4-22)$$

and for emitted phonons the energy balance is

$$h\nu = E_f - E_i + E_p \quad (4-23)$$

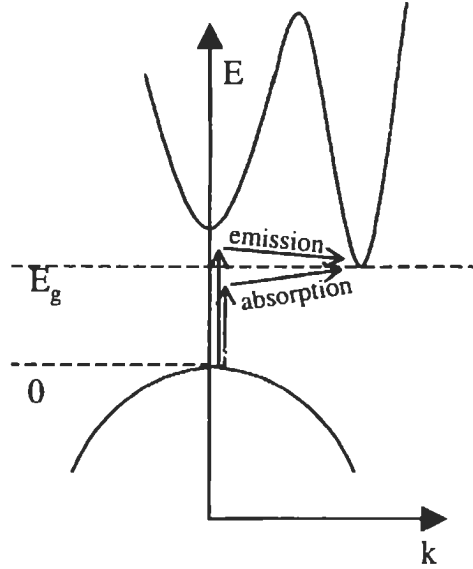


Figure 4-9 Schematic of an absorption event for an indirect transition. A phonon can either be emitted or absorbed to conserve momentum.

Because a phonon is involved in the absorption process, the absorption coefficient is related to the population of phonons, N_p , given by Bose-Einstein statistics as:

$$N_p = \frac{1}{e^{E_p/kT} - 1} \quad (4-24)$$

where E_p is the phonon energy. The absorption coefficient is proportional to $(m_e^*)^{2/3}$ or $(m_h^*)^{2/3}$ which describes the effective density of states in the conduction and valence band, respectively. The absorption coefficient for a transition involving phonon absorption, α_a , is proportional to the phonon population, N_p , and to the excess energy squared, $(h\nu - E_g - E_p)^2$:

$$\alpha_a(h\nu) = \frac{A (m_e^* m_h^*)^2 (h\nu - E_g - E_p)^2}{\left(e^{\frac{E_p}{kT}} - 1 \right)} \quad (4-25)$$

The absorption coefficient contribution for interactions involving the emission of a photon, α_e , scales with $(1+N_p)$ and is also proportional to the excess energy squared, $(h\nu - E_g + E_p)^2$:

$$\alpha_e(h\nu) = \frac{A (m_e^* m_h^*)^{3/2} (h\nu - E_g + E_p)^2}{(1 - e^{-E_p/kT})}, \quad (4-26)$$

where A for both equations above is a constant of proportionality.

4.3.4 Modeling of the Absorption Coefficient

The following steps were used to model the absorption coefficient as a function of strain, and incident photon energy, $h\nu$. The C-code for calculating the absorption coefficient is included in Appendix A.

- 1) The relaxed transition energies between the valence band maximum and the conduction band local X, L, and Γ valley minima are determined as a function of alloy composition either from equations in the literature or by interpolating between values for silicon and germanium.
- 2) Deformation potential theory is used to calculate the shifts and splitting of the valence band maximum and the conduction band X, L, and Γ local minima to determine the change in energy of each of the transitions involving a critical points in the valence band and a local minima in the conduction band. These values are then combined with the relaxed transition energies to yield the strain-perturbed transition energies.
- 3) The absorption contribution of each of the strained transitions is determined from the appropriate equation in Section 4.3.2. The absorption coefficient contributions are then corrected for the reduction in density of states because of degeneracy lifting (scaling absorption contribution to $(m^*)^{2/3}$ for each band). Effective phonon energies from the literature⁷³ for silicon and germanium were assumed characteristic of transitions relating the X and L valley conduction band minima, respectively.
- 4) All of the absorption coefficient contributions are summed to yield the total absorption coefficient.

This model contains two proportionality factors which were determined by fitting the model derived absorption spectrum to the relaxed experimental silicon and

germanium absorption spectrum. The proportionality constants trace back to equations (4-25) and (4-26). Both equations use the same proportionality constant for a given conduction band minima. Thus, the two constants of proportionality correspond to A^X and A^L describing absorption events from the valence band to the X valley conduction band minimum and L valley conduction band minimum respectively.

One of the limitations of this model is its assumption that all the band extrema are parabolic. While this is a reasonable assumption at the bottom of a band, it is not a good assumption for the effective density of states deep within the band. Thus, the calculation of the absorption coefficient will be more accurate for energies just greater than the band gap than for much larger ($h\nu - E_g$) values. In calculating the transition density of states the model also assumes that the material is intrinsic. This is a reasonable assumption since the material in question is in the depleted region of the P-I-N junction. This model being based directly on the calculation of strain perturbed band gap is also limited by the extrapolation and interpolation of constants discussed previously.

4.3.5 Discussion

The absorption coefficient at a particular wavelength can be graphically represented in a form similar to the band gap map. Figure 4-10 shows graphically the absorption coefficient of silicon-germanium as a function of strain and composition at a wavelength of $\lambda = 1.3 \mu\text{m}$. The trends in the absorption coefficient map are very similar to the trends of the band gap. For alloys with germanium fraction less than 0.85, strain (tensile and compressive) is effective in increasing the absorption coefficient. For higher Ge fractions, the absorption coefficient decreases with tensile strain and increases with compressive strain. This occurs because the states in the strain-split band minimum are at too high an energy to participate in electron transitions.

Similar trends are observed for the absorption coefficient at $\lambda = 1.55 \mu\text{m}$ as shown in Figure 4-11. High germanium fractions are needed to detect light at $\lambda = 1.55 \mu\text{m}$. The increase in band gap of pure germanium under biaxial compression in the (100) is of minor consequence at $\lambda = 1.3 \mu\text{m}$ because the absorption coefficient is sufficiently high ($\alpha > 10^4/\text{cm}$). However at $1.55 \mu\text{m}$ the absorption coefficient is smaller and the

compressive strain shifts the direct band gap to higher energies, such that 1.55 μm radiation is no longer as strongly absorbed as in relaxed germanium.

The results of the model suggest that moderate ($\sim 1\%$) tensile and compressive strain can be an effective mechanism by which to lower the bandgap and increase the absorption coefficient. Figure 4-11 shows the absorption spectra for relaxed and 1% compressively strained alloys. Strain is most effective for silicon-rich alloys because the main electron transition involves the strain-split X-valley. Strain is also more effective in increasing the absorption coefficient at photon energies near the band gap of the alloy. For example in Figure 4-11a the difference between absorption coefficient for relaxed and 1% compressively strained $\text{Si}_{0.5}\text{Ge}_{0.5}$ diminishes at shorter photon wavelengths (larger energies). For photon energies that exceed the band gap energy and the conduction band splitting energy ($h\nu > E_g + \Delta E_c$), the strain-split X-valley conduction band does not play a role in increasing the absorption coefficient.

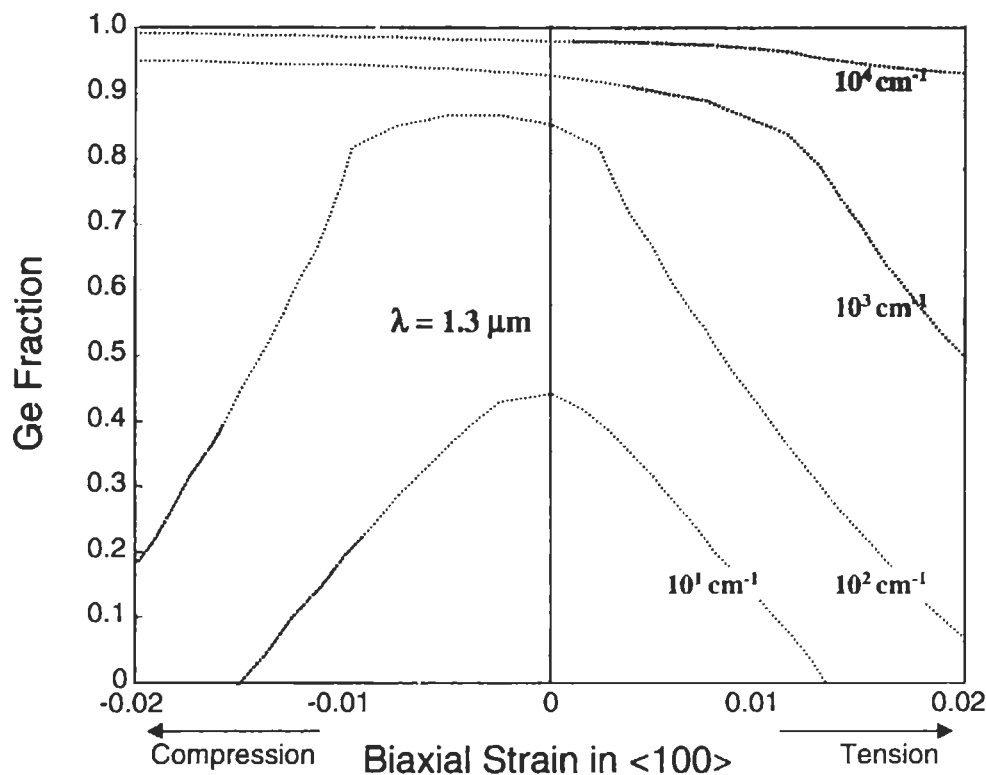


Figure 4-10: Schematic of the absorption coefficient of SiGe as a function of strain and composition at a wavelength of $\lambda = 1.3 \mu\text{m}$. Unshaded areas represent strain and composition combinations that are achievable using strain-balanced superlattice structures.

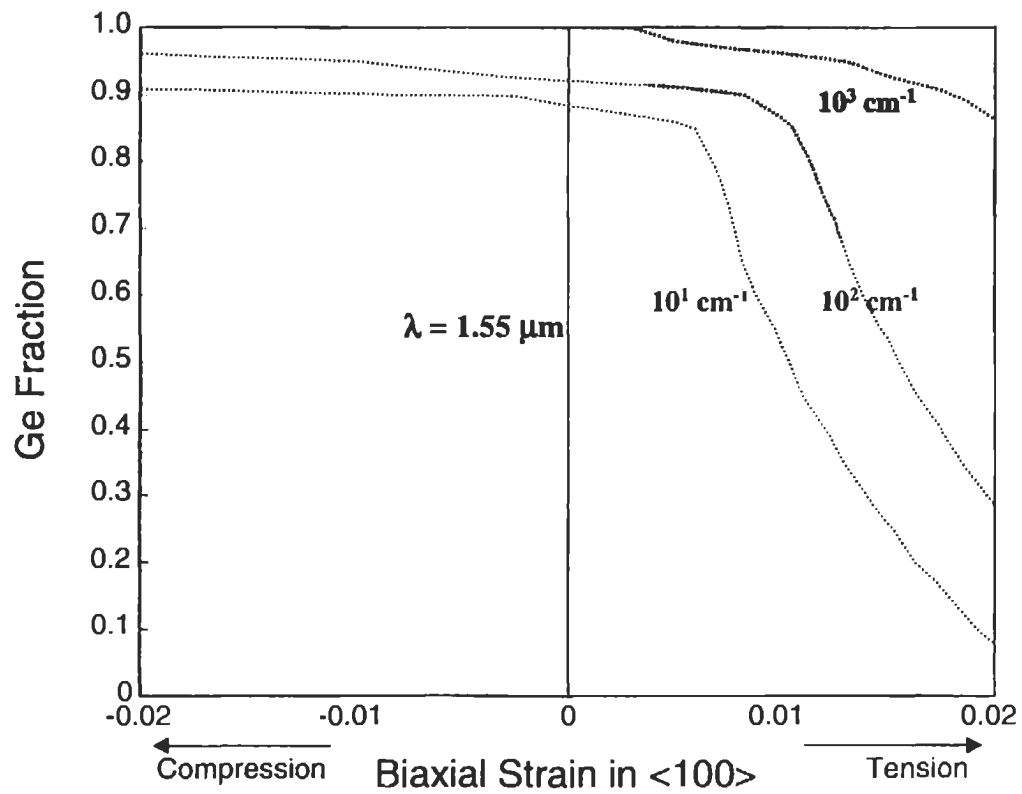


Figure 4-11: Schematic of the absorption coefficient of SiGe as a function of strain and composition at a wavelength of $\lambda=1.55 \mu\text{m}$. Unshaded areas represent strain and composition combinations that are achievable using strain-balanced superlattice structures

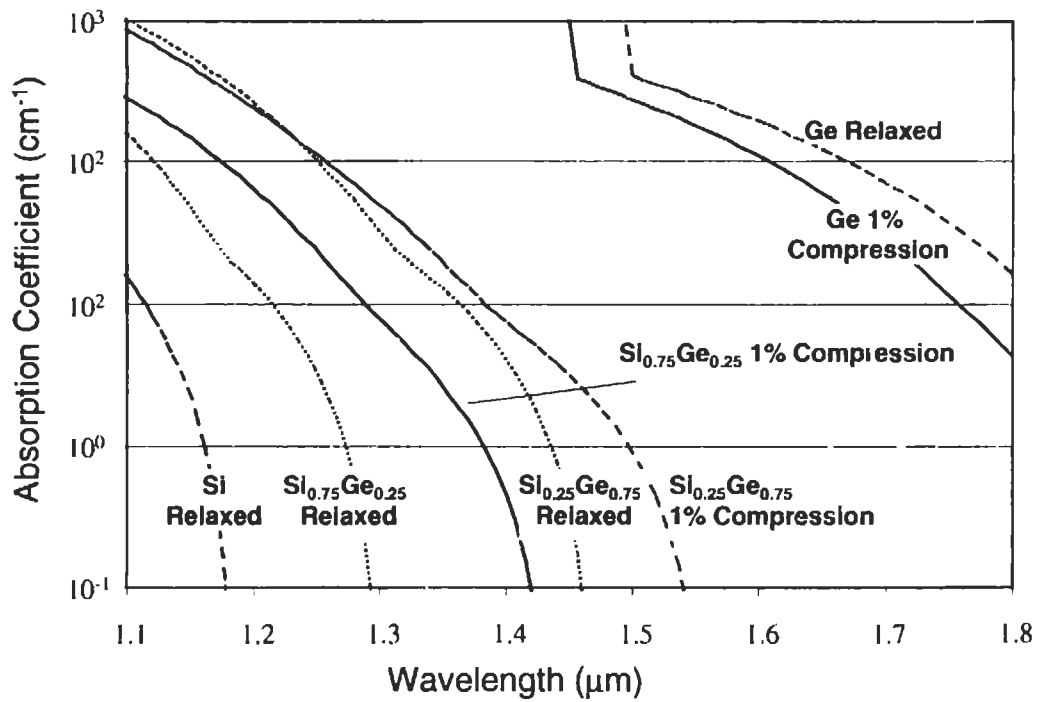
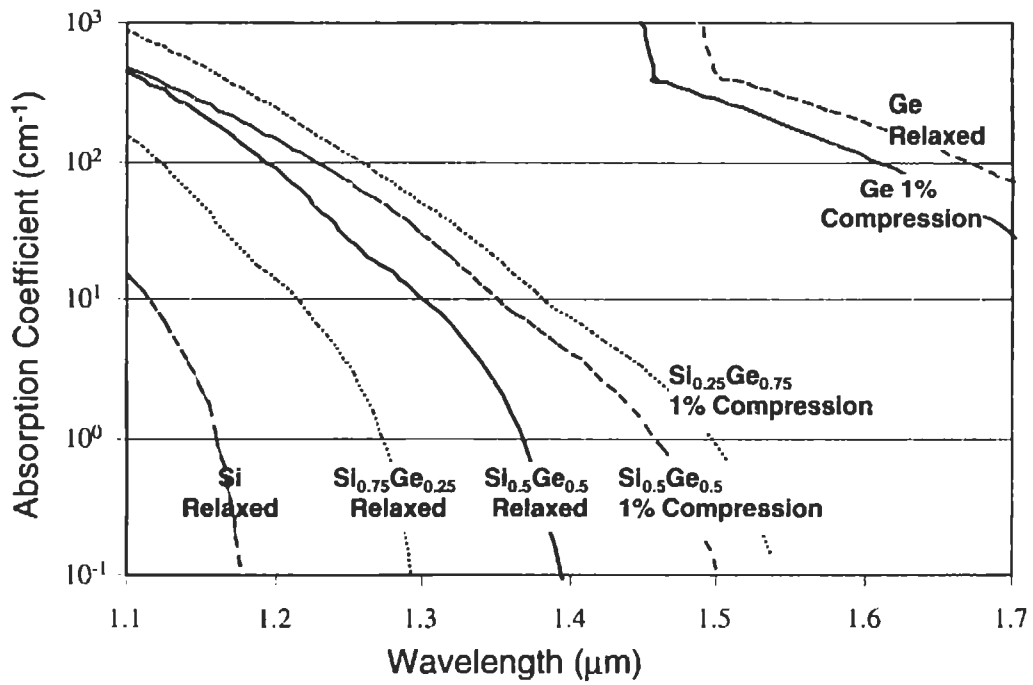


Figure 4-12: The absorption coefficient for various silicon-germanium alloys under different strain conditions.